Pergamon

Geochimica et Cosmochimica Acta, Vol. 68, No. 2, pp. 217–226, 2004

0016-7037/04 $30.00 + .00

doi:10.1016/S0016-7037(03)00375-2

Apophyllite (001) surface alteration in aqueous solutions studied by HAFM

KIRILL ALDUSHIN,[1,2] GUNTRAM JORDAN,[1,*] WERNER RAMMENSEE,[2] WOLFGANG W. SCHMAHL,[1] and HANS-WERNER BECKER[3]

[1]Institut für Geologie, Mineralogie und Geophysik, Ruhr-Universität Bochum, 44780 Bochum, Germany
[2]Institut für Mineralogie und Geochemie, Universität zu Köln, Zülpicher Str. 49b, 50674 Köln, Germany
[3]Institut für Physik mit Ionenstrahlen (Exp. Physik III), Ruhr-Universität Bochum, 44780 Bochum, Germany

(*Received October* 18, 2002; *accepted in revised form May* 14, 2003)

Abstract—Depending on pH and temperature, two different types of surface reactions occur on the apophyllite (001) surface in aqueous HCl-solutions at temperatures from 20 to 130 °C. At low pH, laterally spreading hillocks cover the surface. The hillocks are softer than the pristine surface, chemical analysis shows a depletion in Ca + K, and the spreading velocity of hillocks depends on pH. This indicates a change in chemical bond strength, non-stoichiometric dissolution and a mechanism involving protons. External disturbances such as the AFM scanning tip cause the upper surface layers to peel off revealing that the active sites of hillock formation are between the silicate layers of apophyllite. The observed process can therefore be described by a penetrative ion-replacement reaction which proceeds well below the surface monolayer. By this ion-replacement, the silicate layers eventually become destabilised. The observed reaction, therefore, is equivalent to an incongruent dissolution process. Despite structural similarities, this process is only superficially similar to the ion-exchange occurring in clay minerals or zeolites. In these minerals, the structural backbone is not destabilized. At a more neutral pH and high temperatures, step retreat and etch pit formation can be observed on the apophyllite (001) surface thus indicating a more congruent dissolution mechanism.

1. INTRODUCTION

In situ observations of surface processes on silicate minerals are important for the interpretation and understanding of geochemical processes such as mineral formation or the weathering of rocks. In this work, we present the results of *in situ* investigations of the behavior of the apophyllite (001) surface in aqueous solutions. Although this hydrous sheet silicate is less common than micas or clay minerals, the study of this mineral surface can give very useful insights in the interpretation of processes taking place on many other silicates.

Apophyllite [$KCa_4Si_8O_{20}(F,OH) \cdot 8H_2O$] is frequently found associated with zeolites in rocks affected by low temperature alteration processes. Further, apart from the environment of formation, apophyllite resembles many zeolites, e.g., in structure, low specific gravity and the ability to release water under heating (Marriner et al., 1990). Nevertheless, apophyllite is a sheet silicate and structurally and chemically it is very close to clays and micas. Hence, apophyllite is expected to exhibit reactive properties similar to those of both zeolites and phyllosilicates.

Apophyllite is tetragonal, space group: P 4/mnc, a = 8.96 Å, c = 15.8 Å (Colville et al., 1971). Like other phyllosilicates, it has a layered structure, where the tetrahedral silicate layers alternate with layers of Ca, K, F and OH. However, in contrast to other phyllosilicates, the silicate layers of apophyllite are composed of interconnected four- and eight-membered rings, with the terminal, non-bridging tetrahedral apexes of the four-membered rings alternatingly pointing up and down along the c-direction (Fig. 1). The terminal tetrahedral apexes of adjoining layers oppose each other and form via the interim Ca-ions a ≡Si-O-Ca-O-Si≡ type bonding, thus making a kind of framework with alternating voids and, therefore, resembling a zeolite structure. Nevertheless, the three dimensional ≡Si-O-Si≡ type bonding in zeolites provides a much stronger linkage than the linkage via Ca in apophyllite. The structure of clays and micas consists of silicate layers, which are strongly joined by octahedrally coordinated divalent or trivalent cations into packets. Between these packets are layers of exchangeable cations. Most clays are characterized by cation exchange capacity and the ability to adsorb water, which sometimes causes these minerals to swell. In zeolites, which also exhibit ion exchange and water adsorption properties, these processes occur without swelling because of the large cavities and strong bonds between the tetrahedra.

One of the most effective methods for *in situ* surface studies is atomic force microscopy (AFM). This method allows the direct observation of mineral surfaces in air, solution or vacuum and has been proven as a powerful technique for the investigation of morphologic changes during mineral dissolution, precipitation and growth (e.g., Nagy and Blum, 1994; Stipp et al., 1994; Teng and Dove, 1997; Bosbach et al., 1998; Higgins et al., 2002). The original design of AFM instruments was limited to performing studies at ambient conditions. For this reason, most AFM studies of surface reactivity so far concern minerals which show reaction rates fast enough to be detectable within an appropriate time range of AFM imaging, such as many carbonates and sulfates (e.g., Hillner et al., 1992; Hall and Cullen, 1996; Jordan and Rammensee, 1998; Shiraki et al., 2000; Astilleros et al., 2002). However, for most silicate-water interface reactions, the kinetics is too slow at ambient conditions to allow its *in situ* investigation by AFM within a reasonable period of time. Recently, this constraint has been overcome by the development of a hydrothermal AFM (HAFM, Higgins et al., 1998). This device enables *in situ* AFM

* Author to whom correspondence should be addressed (guntram.jordan@ruhr-uni-bochum.de).

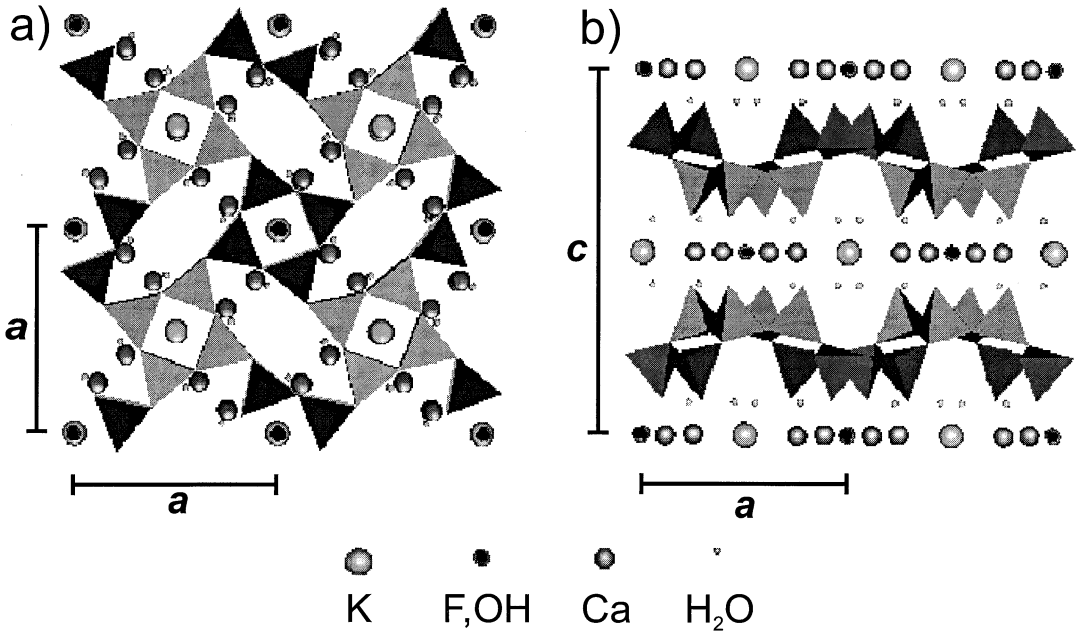

Fig. 1. Structure of apophyllite: a) the projection along *c* shows four- and eight-member rings in (001), with 4-member rings alternatingly pointing up (dark tetrahedra) and down (light tetrahedra) the *c*-direction; b) view along [100] shows layers of cations, hydroxyls, and fluorine ions between the silica layers.

experiments at hydrothermal conditions, i.e., above the ambient boiling point of water.

Many investigations have been conducted to study the dissolution of zeolites, clays, and micas (e.g., Newman, 1970; Sposito, 1984; Kalinowski and Schweda, 1996; Zysset and Schindler, 1996; Charistos et al., 1997; Malmström and Banwart, 1997; Rufe and Hochella, 1999; Huertas et al., 1999; Rivera et al., 2000). There are also some AFM data about the dissolution and interlayer exchange processes of these minerals. For example, it has been shown that the natural zeolite heulandite dissolves in acidic solution (0.2 N H_2SO_4) by pit formation and in alkaline solution (0.1 N NaOH) isolated islands are left behind (Yamamoto et al., 1996). Two smectite minerals – hectorite and nontronite – dissolve at pH 2 at the crystal edges, with the basal surface remaining unreactive during the timescale of the experiment (Bosbach et al., 2000; Bickmore et al., 2001). Hochella et al. (1998) observed the delamination and/or recombining of clay-size phlogopite particles while establishing an equilibrium thickness in Na^+ containing solutions.

The behavior of apophyllite in acidic solutions was studied before by batch methods and X-ray diffraction. For example, Frondel (1979) reported the formation of crystalline silica hydrate Silica-AP ($H_2Si_4O_9$) by the decomposition of apophyllite in acidic solution (HCl). Lagaly and Matouschek (1980) observed the formation of H-apophyllite ($H_8Si_8O_{20}xH_2O$) after the pretreatment of apophyllite in acidic solution. According to these authors and Sogo et al. (1998) both of these hydrates have the fundamental silica sheet structure of apophyllite. Theodossiu et al. (2001) reported surface amorphization of apophyllite due to acidic attack and therefore a total collapse of the local crystal structure. The most complete investigation of apophyllite dissolution was conducted by Cave (2002). This author found that apophyllite dissolves non-stoichiometrically in acidic solution with a preferential loss of interlayer cations and that dissolution approaches congruency in the neutral pH range. At neutral pH, dissolution rates of apophyllite are faster than those of kaolinite or muscovite; this has been attributed to an increased strain on the bonds in the four-membered silicate rings (Cave, 2002).

Here, we present *in situ* investigations of the alteration of the apophyllite (001) surface in aqueous solutions studied by HAFM at temperatures from 20 up to 130 °C and pressures from 1 up to 35 bar in solutions ranging from pH 1.5 to 5.6. Our primary objectives were to study the mechanisms and kinetics of surface reactions of apophyllite in aqueous solutions and to compare these mechanisms with dissolution of clays, micas and zeolites at appropriate conditions.

2. EXPERIMENTAL

Apophyllite shows some variations in composition, specifically the fluorine content, and can be considered as a solid-solution between the two end members: fluorapophyllite $KCa_4Si_8O_{20}F \cdot 8H_2O$ and hydroxyapophyllite $KCa_4Si_8O_{20}(OH) \cdot 8H_2O$ (Dunn et al., 1978). In our experiments, we used apophyllite from Poona (India) where it is often accompanied by heulandite. The electron microprobe analysis of our samples (Table 1) revealed that the crystals used are fluorapophyllites.

Because of its perfect cleavage parallel to (001) and well-developed crystals, apophyllite is suitable for AFM studies. Transparent, colorless crystals were cleaved by a knife immediately before affixing them in the fluid cell by a titanium wire and immersing them into the solution. The titanium wire allows the crystal to be affixed without any adhesive. The samples used were 0.2 - 1.5 mm thick, the size of the (001) surface was about 5–15 mm^2. After the fluid cell was filled with solution, the cell was then closed, pressurized, and heated for hydrothermal experiments. The duration of experiments was up to 15 h.

Solutions were prepared using high purity deionized water (resistivity: 18 MΩ cm); the pH values of solutions were adjusted to pH 1.5–5.6

Table 1. Electron microprobe analysis of the apophyllite samples used.

	Compound, wt. %			Atomic %	
	average (n = 100)	std. dev.		average	std. dev.
SiO_2	51.451	0.263	Si	13.168	0.123
Al_2O_3	0.016	0.014	Al	0.005	0.004
K_2O	5.032	0.097	K	1.643	0.035
CaO	24.456	0.207	Ca	6.706	0.081
F	2.371	0.067	F	1.919	0.055
H_2O	16.669	0.282	H	28.458	0.331
			O	48.101	0.138
Total	99.995			100.000	

at room temperature by adding HCl. The flow rate of the solution through the fluid cell was set to values between 0 and 14 μL/s.

All *in situ* measurements were carried out using a contact mode HAFM which was constructed in our laboratories. This device allows *in situ* measurements of the solid-liquid interface at pressures up to 50 bars and temperatures up to 170 °C to be made. We used uncoated Si-cantilevers with integrated tips (spring constant: 0.1–0.3 N/m). *Ex-situ* AFM images were obtained using a TopoMetrix TMX 1010 AFM operating in contact mode.

Rutherford backscattering spectrometry analysis was conducted to find out the chemical composition of the near-surface region of the samples after their treatment in acidic solution. The RBS spectra were measured with the 2 MeV single charged He-beam of the 4MV Dynamitron-Tandem of Ruhr-Universität Bochum with a beam intensity of about 10 nA. The backscattered particles were measured at an angle of 170 ° by a Si-detector with a resolution of 15 keV. The energy of the backscattered particles depends solely on the masses of the elements according to the kinematics of the scattering process. For layers below the surface, the signals are shifted towards lower energies due to the energy loss of the particles in the sample causing step-like structures in the spectrum. Depth information can be obtained, using the well known energy loss data for ions in matter and the density of the investigated material. The relative sensitivity for the elements is proportional to the square of the atomic number. The method, thus, is more sensitive to heavier elements for which traces of less than one atomic layer at the surface can be detected.

The spectra were analysed using the program RBX (Kotai, 1994). This program calculates the shape of the spectra based on the experimental conditions and the stoichiometry of the sample as input parameters. The sample can consist of several layers and a changing stoichiometry within a layer can be described by an error function representing the concentration of a species varying with depth. The simulated spectra are then compared to the measurement until a sufficient fit is achieved.

3. RESULTS

3.1. Experiments at pH 1.5 - 3, T = 20 °C, P = 1 bar

20 - 30 min after the injection of the solution with a pH of 2.9–3, the formation of small hillocks on the surface of the sample can be observed. The hillocks are usually square shaped (reflecting the tetragonal symmetry), their height is about 0.3 - 0.4 nm, they have a flat surface, distinct boundaries, and an identical orientation (Fig. 2a). The areal density of the hillocks is 2–20 μm^{-2}. The hillocks spread with time in lateral directions and finally form a layer on the surface. At pH 3, the spreading rate measured perpendicular to the straight bound-

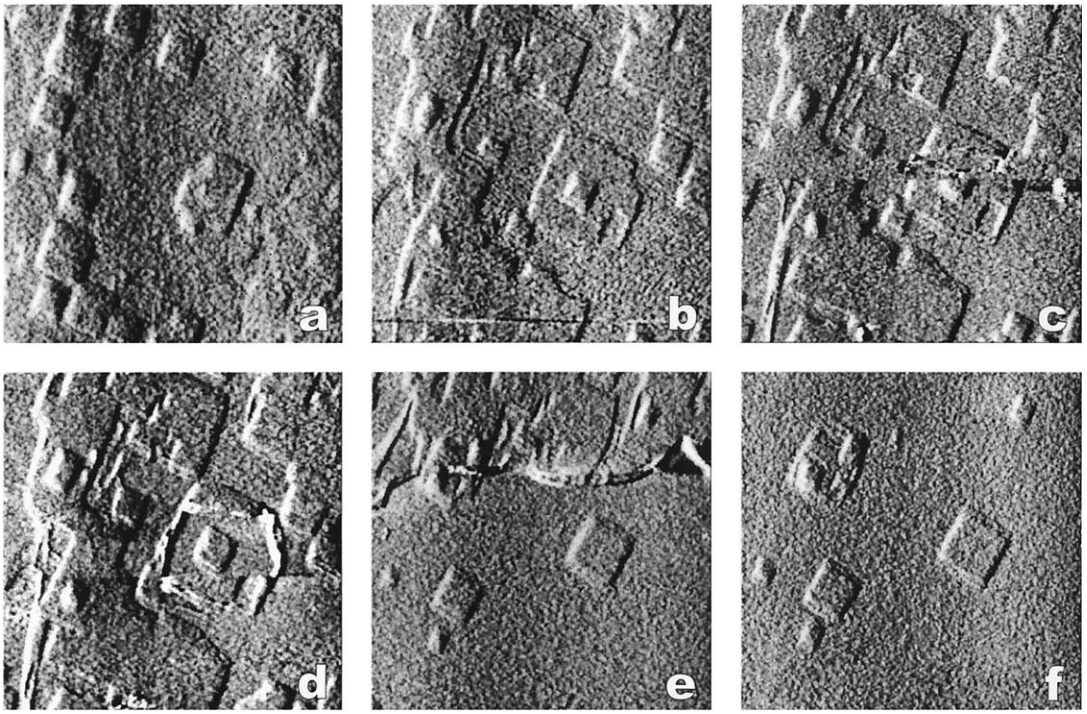

Fig. 2. Formation of square hillocks on the surface and their subsequent peeling (pH 3, T = 20 °C, P = 1 bar): a) after 180 min exposure to acidic solution: first generation of hillocks; b) 60 min later; formation of a second generation; c) 70 min after the first image; start of peeling off the uppermost surface layer; d) 85 min; and e) 140 min after the first image; peeling off the upper layer progresses; f) 150 min after the first image; new surface only with hillocks of second and third generation. Scan field 2 $\times$2 μm^2.

aries of hillocks is 1.8 ± 0.3 nm/s. In Figure 2b, the formation of a second generation of hillocks can be observed. The second generation of hillocks preferentially occurs in the centers of the hillocks of the first generation. They have the same height, orientation, and lateral spreading rate as the first generation. Later, the formation of a new, third generation of hillocks can be observed. The sequence of the formation of hillock generations is limited by a significant additional process. After the formation of the 2nd to 4th generation, the upper layer peels off the surface by the continuously scanning tip (Fig. 2c-e); the process is often accompanied by an accumulation of the peeled material at the margins of the scan fields. This shows that the upper layer becomes unstable after some period of time. The height of this peeled-off layer is about 0.7 - 0.9 nm in areas without hillocks and 1.0 - 1.2 nm in areas where the hillocks have already formed (measured at steps of partially peeled-off layers).

After the removal of the upper layer (Fig. 2e-f), it can be seen that the second generation hillocks still remain and spread on the surface, whereas the hillocks belonging to the first generation have been removed along with the peeled off layer. In Figure 2f the formation of the third generation of hillocks can be observed. The next peeling process will remove the upper layer along with the hillocks of the second generation and the hillocks of the third generation will remain on the surface.

These observations show that formation of hillocks is not a growth process taking place *on* the surface. If a formation of a new phase was taking place *on* the original surface, one would expect that the peeling process would remove the youngest generation of hillocks. Here, the opposite behavior can be observed: peeling off the surface layer removes the oldest generation. Therefore, the formation of hillocks occurs not on the surface, but underneath or, to be more exact, under the first one or two silicate layers. After the formation of the first generation, the formation of the second is initiated underneath the first generation - the younger the hillock generation, the deeper it actually is located. This process is illustrated schematically in Figure 3. Since the peeled, hillock-free layer has a height of about 0.7 - 0.9 nm (approximately corresponding to one half of the c-lattice constant of apophyllite), each layer in the sketch corresponds to one silicate layer (Fig. 3a). A process taking place underneath the upper silicate layer provokes rising of the silicate layer and, as a result, we observe a hillock on the surface (Fig. 3b). This hillock has a constant height and spreads laterally. The same process recurs under the second silicate layer (Fig. 3c). Since the size of the later formed hillock is smaller, the second generation hillock is apparently above the first one. Finally, peeling off the upper layer removes the first generation and only the hillock of the second generation remains (Fig. 3d-e).

The hillocks are softer than the pristine apophyllite surface. Applying even medium loading forces (such as 2.5 ± 0.5 nN) causes a considerable decrease in the hillock's height. The surface of the compressed hillocks is almost on the level of the unaltered surface, leaving visible only the outline of the square shaped hillocks (Fig. 4a). However, scanning with high loading forces usually induces peeling off the upper surface layer. Decreasing the loading force to 1 ± 0.3 nN causes an increase in the height of the hillocks (Fig. 4b). By further reducing the loading forces to the limit (0.4 ± 0.2 nN), the hillocks show their maximum height (Fig. 4c).

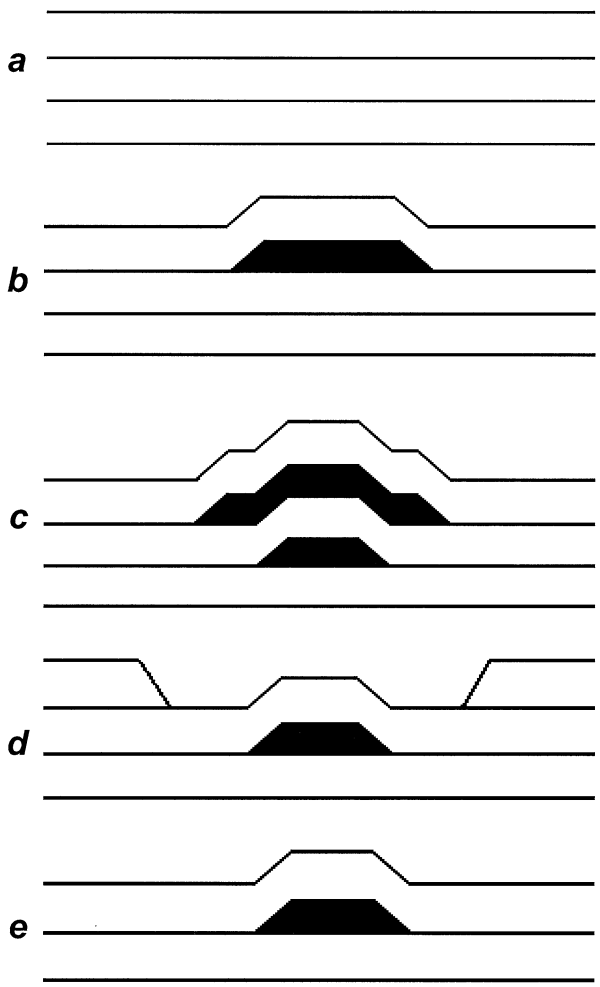

Fig. 3. Scheme of the hillock formation on the surface: a) atomic layers of the mineral; b) formation of the first generation hillocks; c) the same process recurs under the second silicate layer; d) peeling process removes the upper layer; e) only the second generation hillock remains on a surface.

Decreasing the pH-value of the solution from 3 to 2.5 - 1.5 causes further interesting features of the apophyllite-water interface. As in the experiments at pH 3, all hillocks of one generation have roughly a square shaped outline in the same orientation, and have a tendency to form an uniform layer. However at lower pH values (Fig. 5), the hillocks spread more rapidly (pH 2: 8.7 ± 1.3 nm/s). Additionally, as can be seen from Figure 5c-d, the second generation hillocks are rotated relative to the hillocks of the first generation by an angle of about 25 ± 3°. Furthermore, the hillocks of the third generation have again the same orientation as the hillocks of the first generation (Fig. 5e-f). Thus, the orientation is toggled back and forth in successive generations.

Exposure of the sample to pH 2 for 5 h without scanning leads to the formation of an unstable and soft layer with a thickness of about 15 - 20 nm. Scanning of this surface results in a removal of this thick soft layer and uncovers a hard surface on which the formation of the hillocks continues.

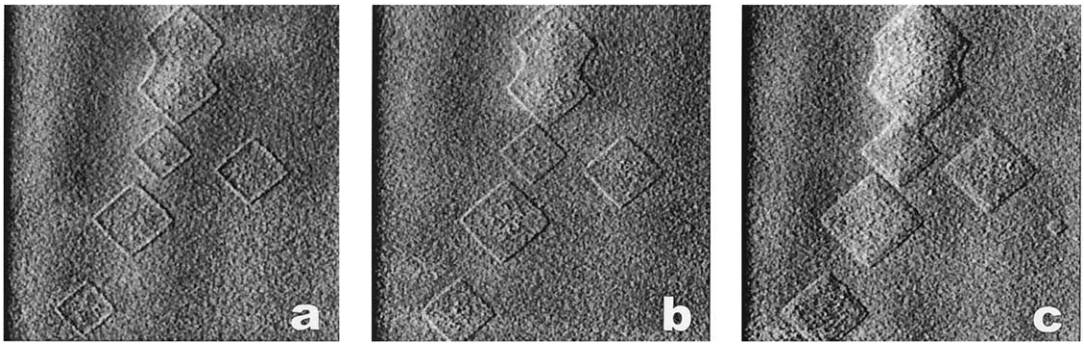

Fig. 4. Influence of different loading forces (F_L) on the hillocks height: a) $F_L = 2.5 \pm 0.5$ nN: decrease in the height of hillocks; b) $F_L = 1 \pm 0.3$ nN: increasing height of the hillocks; c) $F_L = 0.4 \pm 0.2$ nN: the hillocks show the maximum height (3.5 - 4 Å). Scan field 2 $\times$2 μm^2.

In situ observation further revealed that the rate of lateral spreading of the hillocks does not depend on their size. The rate remains roughly constant from the time when the hillock becomes visible until its coalescence with adjacent hillocks (Fig. 6).

Apart from the formation of hillocks, rising of the silicate layer could also be found at cleavage steps on the basal surface at all pH values from 3 to 1.5. The spreading rate of this process is comparable to the hillock spreading (Fig. 7).

3.2. Experiments at pH 3, T = 40–100 °C, P = 10 - 35 bar

The formation of hillocks can also be observed at higher temperatures (40–100 °C) and higher pressures (10 - 35 bar). In experiments at high temperatures we used solutions with pH values of 2.9 - 3. As can be seen in Figure 8, the temperature significantly influences the spreading rate: at pH 3 and 20 °C the rate is about 1.5 nm/s, at 100 °C it increases to about 200 nm/s. In spite of such high rates the hillocks generally keep their square forms, usually with rounded corners, although in some cases, especially at 100 °C, they may appear almost completely round. At these conditions, scanning with even minimum loading forces leads to an almost immediate peeling of the surface. Therefore, the observation of the development of hillocks is hampered. From the temperature dependence of the spreading rate an apparent activation energy for the growth of hillocks can be

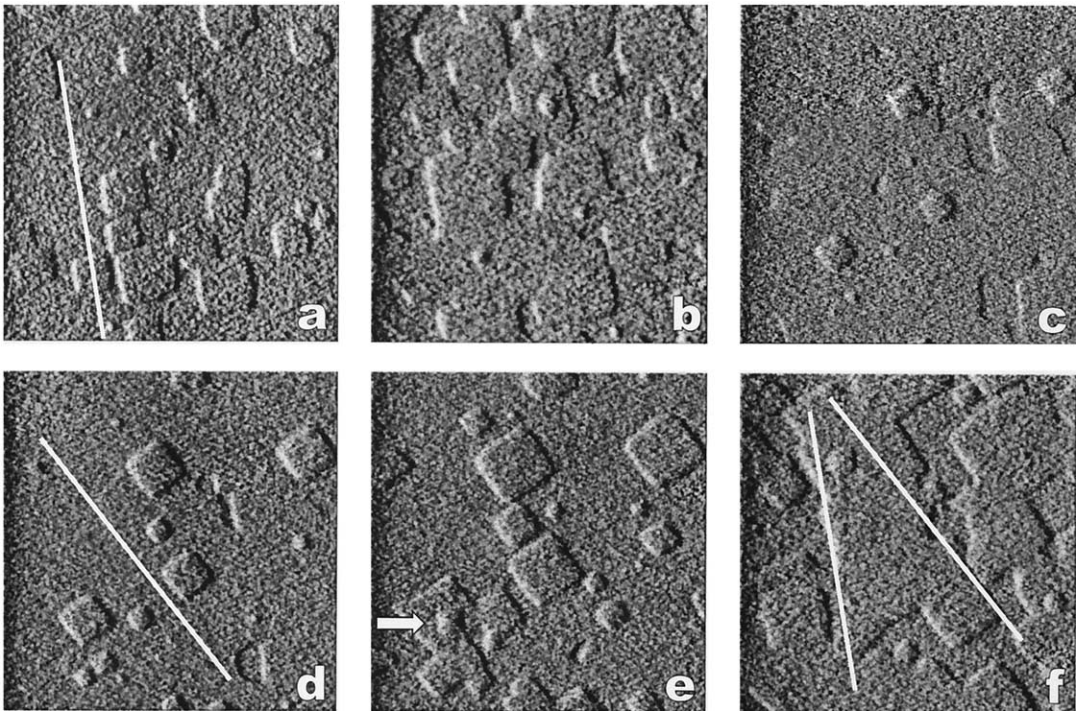

Fig. 5. Effect of lower pH values (pH 2, T = 20 °C, P = 1 bar): a) hillocks of the first generation; b - d) formation of the second generation hillocks and their spreading. The second generation is rotated by an angle of about 25 ±3°; e) formation of the third generation; f) orientation of third generation hillocks is identical to the orientation of the first generation. Scan field 1.5 $\times$ 1.5 μm^2.

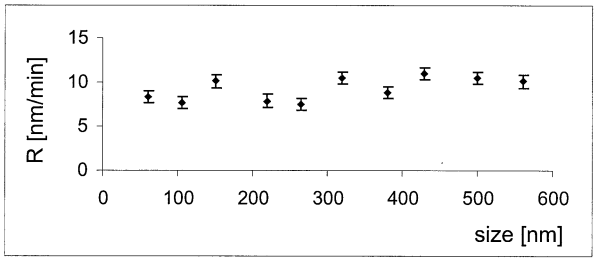

Fig. 6. Rate of lateral spreading of hillocks versus hillock size at pH = 2 and T = 20 °C, P = 1 bar.

calculated. Based on the data shown in Figure 8, this activation energy is 57 ± 2 kJ/mol.

The rate of hillock spreading also depends on the pressure in the system. The pressure dependence is weaker than the temperature dependence and has the inverse correlation: increasing pressure causes the rate of spreading to decrease (Fig. 9). For solutions with pH 2.9 at T = 20 °C, the spreading rate is about 3 nm/s at atmospheric pressure and decreases to about 1.5 nm/s at P = 35 bar.

3.3. Experiments at pH 5.6, T = 110–130 °C, P = 10 bar

The experiments in solutions with a more neutral pH (5.6) at high temperatures revealed a significant change in reaction mechanism on the (001) surface of apophyllite: after increasing temperature to 110–130 °C, dissolution of the (001) surface of apophyllite occurs by step retreat (Fig. 10). The height of steps in most cases ranges from a few nanometers to several tens of nanometers - usually more than one c-lattice constant. The steps are very rough. *Ex-situ* measurements showed that after a pretreatment at high-temperature, the sample surface was covered by large square etch pits (Fig. 11), making it reasonable to assume that the retreating steps in the *in situ* images belong to terraces emanating from such pits. Based on the etch-pits, the dissolution rate at these conditions (130 °C, 10 bar) has been estimated to be 5×10^{-7} mol/m^{2}s.

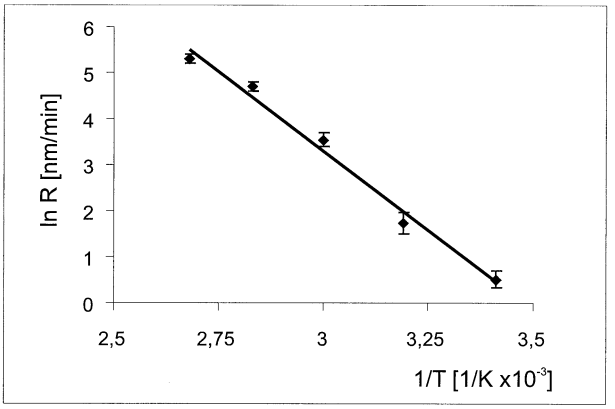

Fig. 8. Influence of temperature on the rate of hillock spreading at pH = 3, P = 35 bar.

3.4. Rutherford Backscattering (RBS)

To obtain information about the chemical composition of the near surface region of apophyllite, Rutherford Backscattering analysis (RBS) has been performed. Two kinds of samples have been used: *(i)* apophyllite (001) surface pretreated by immersing the crystal in a pH 2 HCl-solution for 10 h at room temperature and *(ii)* freshly cleaved apophyllite (001) surface. Figure 12a shows the RBS spectrum of the freshly cleaved surface of apophyllite and a superimposed simulated spectrum based on the atomic ratios as obtained by electron microprobe analysis (see Table 1). Figure 12b shows the comparison between the RBS surface spectrum of the pretreated sample and the simulated spectrum of the pristine surface of the freshly cleaved crystal. The content of F^- in apophyllite is too low to definitely judge any changes in its amount due to the treatment. However, the comparison of the spectra clearly reveals a depletion of the elements calcium and potassium in the near surface region of the pretreated crystal. Simulated spectra can be fitted to this experimentally obtained data by varying the atomic ratios of the elements as a function of depth. Figure 12c shows the concentration of Ca + K (in formula units) with

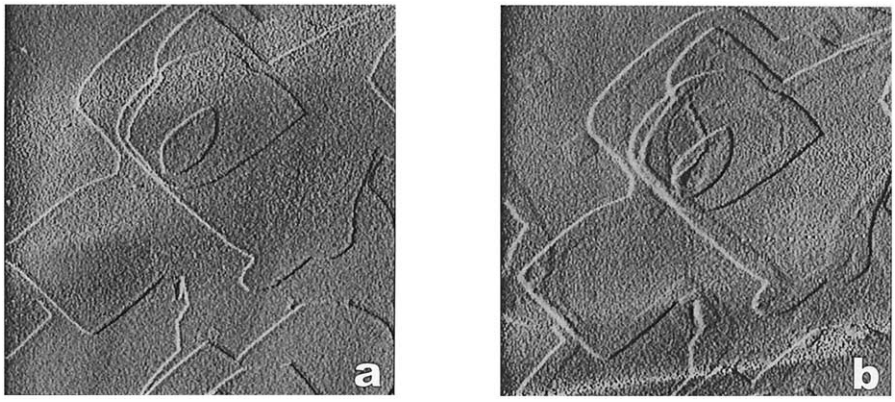

Fig. 7. Swelling of cleavage step edges and formation of square hillocks: a) unaltered surface with cleavage steps after 15 min in water (pH = 5.6, T = 20 °C, P = 1 bar); b) the surface area (slightly shifted) after exposure for 20 min in acidic solution (pH = 1.5, T = 20 °C, P = 1 bar). Scan field 4.5 × 4.5 μm^2.

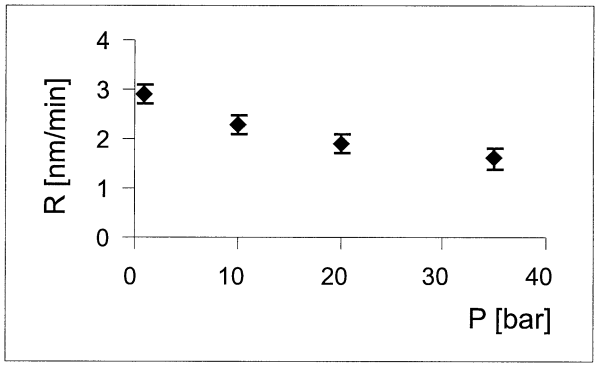

Fig. 9. Rate of lateral spreading of hillocks versus pressure in the HAFM at T = 20 °C and pH = 2.9.

increasing depth in the near surface region of the pretreated crystal. Depletion of Ca + K is observed to a depth of 250 ± 20 nm. The error is estimated from the uncertainty in determining the depth at which the concentration reaches a constant value in Figure 12c, other experimental errors are smaller and here negligible. Below 250 nm the concentration of Ca + K is about 8 atomic %, which is in accordance with our electron microprobe analysis of untreated apophyllite (Ca + K = 6.71% + 1.64% = 8.35%). With decreasing depth this value decreases to 1.53% at the surface. While Ca + K concentrations are clearly reduced in the near surface region, Si does not show such a depletion, indicating more or less intact silicate layers.

4. DISCUSSION

To understand the behavior of the apophyllite (001) surface in acidic solution, we have to consider three basic observations:

Fig. 10. Deflection image of retreating steps on the (001) surface of apophyllite at 130 °C (pH = 5.6, P = 10 bar; steps are stepping down from left to right). The morphology of the steps is rough, their height is about a few nanometers. Scan field 6 × 6 μm^2.

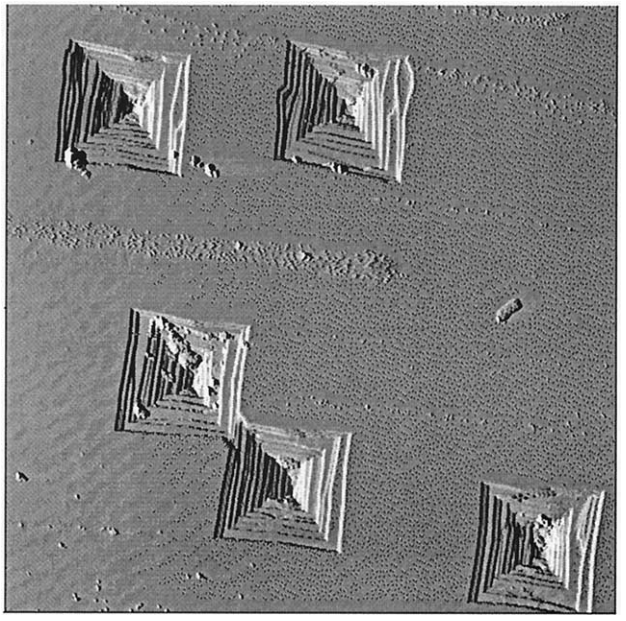

Fig. 11. *Ex-situ* AFM image of etch pits developed on the (001) surface of apophyllite after 3 h at 130 °C (pH = 5.6, P = 10 bar). Scan field 100 × 100 μm^2.

(i) RBS indicates a change in chemical composition in the near surface region. The results show a decrease in the (Ca^{2+} + K^+) concentration. Release of these cations requires charge compensation, which may only be partially achieved by removal of F^-.

(ii) The observed spreading rate of the hillocks increases with decreasing pH. Therefore, the surface reaction leading to the formation and spreading of the hillocks is clearly proton promoted, making it reasonable to expect protons compensating for the loss of interlayer cations, and, moreover, making it likely that protonation drives the removal of interlayer cations into the solution.

(iii) The formation of hillocks, or "localized swelling," along with the fact that the surface of the hillocks becomes unstable and is easily removable by the AFM tip, suggests that there is a profound change in the nature of interlayer coupling. This change may possibly be related to an attachment of protons to the terminal oxygens of the silicate sheets.

Directly at the surface of the pretreated sample, RBS indicates a concentration of Ca^{2+} + K^+ of 1.53 atomic %. This value is very close to the content of K^+ in the pristine apophyllite. Due to the close atomic weights of Ca and K, it is not possible to distinguish between these two elements by RBS. The result therefore may suggest the possibility that only Ca^{2+} is actually released while K^+ remains attached. However, there is no obvious reason for such a preferential release of Ca^{2+} over that of K^+ ions.

Experiments investigating the long term reaction of the surface region of apophyllite with aqueous solutions were conducted by Cave (2002). As it was shown by this author, SEM-EDX analyses of apophyllite immersed in pH 2 solution for 4 weeks reveal only Si and O and no detectable K, Ca, or

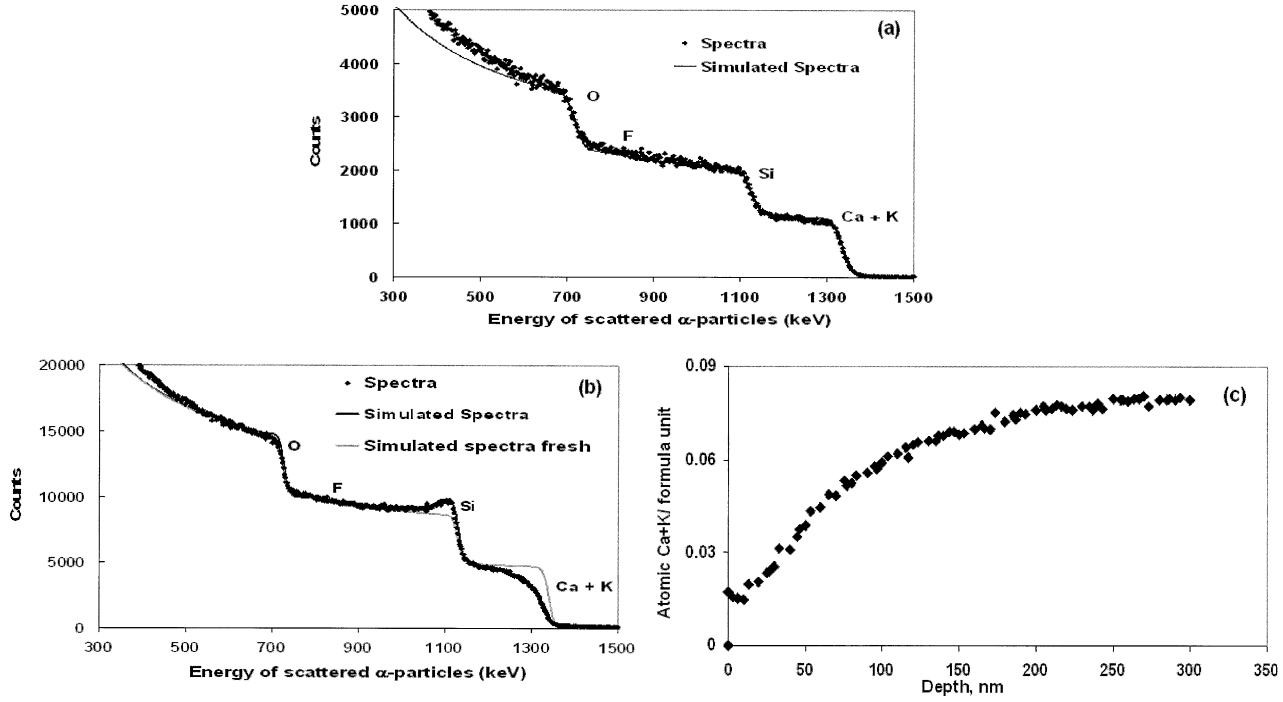

Fig. 12. RBS-spectra of the near surface region on the (001) surface of apophyllite: a) RBS spectrum of a freshly cleaved surface superimposed by a simulated spectrum based on the electron microprobe analysis (see Table 1). b) RBS surface spectrum of a sample immersed in pH 2 at room temperature for 10 h superimposed by a simulated spectrum of the reacted surface. Additionally for comparison, a simulated spectrum of a freshly cleaved surface is inserted. c) Change of Ca + K concentration with increasing depth. The depth of the altered layer is about 250 ± 20 nm.

F in the outer layers of the mineral residue. Other studies of the system apophyllite - acidic solutions (batch dissolution and X-ray experiments) further revealed that the reaction leads to the formation of a crystalline silica hydrate residue by selectively releasing the Ca, F, OH and K ions from the interlayer space (Frondel, 1979; Sogo et al., 1998).

Thus both the long term and the present short term investigations show that Ca^{2+}-ions are released from the surface region. Since in the apophyllite structure the silicate layers are linked together by Ca^{2+}-ions (other ions play an inferior role in interlayer linkage), release of Ca^{2+}-ions and the formation of silanol groups by H_3O^+ entering the interlayer space is likely to cause a reduction of bonding forces between the silicate layers. Removal/replacement of Ca^{2+}-ions, therefore, is likely to cause an increase in the distance between the layers, which may explain the hillock formation. It is further likely that additional H_2O molecules enter the interlayer space as the swelling occurs, but there is no direct evidence for hydration. The swelling can be easily suppressed by applying loading forces in excess of ~ 3 nN on the AFM tip. This gives an idea of the magnitude of the forces between the disjoined layers.

The active role of H_3O^+ is emphasized by the observation that in the range of pH values studied (3 - 1.5), the rate of hillock spreading rises by an order of 0.6 from approximately 1.7 nm/min at pH 3 to 20 nm/min at pH 1.5 at room temperature (Fig. 13). Furthermore, an increasing proton concentration continuously changes the orientation of the straight reaction front in subsequent layers. While the alternating back and forth rotation of the hillocks can be explained by the glide planes in apophyllite structure, we speculate kinetic reasons being responsible for the rotation itself. At the straight reaction front, the rate of exchange reaction might be different in opposing directions along the front. At decreasing pH this anisotropy may increase causing an increased rotation. A similar effect was proposed to be responsible for the step rotation at magnesite etch pits (Jordan et al., 2001). Also on apophyllite, rotation of etch pits has been observed (Joshi and Ittyachen, 1967). These authors have etched the basal cleavages of apophyllite crystals at different concentrations of ammonium bifluoride solutions and observed etch pits rotating up to 45°. The rotation has been attributed to differences in etch resistiv-

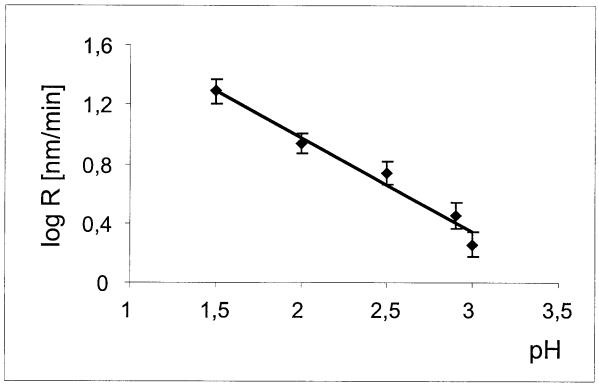

Fig. 13. Influence of solution pH to the rate of hillock spreading. The slope of the linear regression is 0.6.

ity. Pande and Vadrabade (1990) investigated HF-etching of the basal surface of apophyllite using different concentrations of ammonium fluoride as an inhibitor. These authors attributed the observed change in orientation of the pits to different adsorption sites of aqueous complexes on apophyllite.

Starting from a nucleus-like point, the hillocks spread laterally at straight boundaries until a layer is formed by coinciding hillocks. The same process further affects successive layers. Our observations reveal that the thickness of the altered layer can reach several tens to hundreds of nanometers within a few hours in acidic solution at room temperature. Assuming comparable long term behavior after 4 weeks, the thickness of this layer at pH 2 can reach about 1000 nm (Cave, 2002). Since the hillocks are often nucleating at the same lateral position in successive layers, it can be assumed that the point of nucleation is related to anomalies in the crystal structure like linear defects.

As we mentioned above, the depth of the altered layer, as determined by RBS is about 250 nm after 10 h at pH 2, while according to the AFM *in situ* observations at similar conditions, the depth of this layer should be about 40 - 50 nm. This discrepancy can be explained by the presence of steps on the cleaved surface. Due to additional ion replacement at cleavage steps, a rough stepped surface reacts as a whole much faster than the flat surface. The AFM measurements require atomically flat surface and cover the area not more than 40×40 μm^2, whereas the RBS beam in our experiments covered the area of 0.5×0.5 mm^2.

At high temperature and low pH, the silicate layers become very unstable, causing the silicate layers to peel off rapidly. This process impedes acquisition of quantitative kinetic data at these conditions by AFM. For comparison, Cave (2002) revealed that the average rate of fluorapophyllite dissolution at 25 °C and pH = 2 is 3.5×10^{-10} mol/m^2s, and it decreases to 3×10^{-11} mol/m^2s at pH = 4.

According to Sogo et al. (1998), the risen silicate sheet has the same fundamental structure as the sheet of apophyllite. After prolonged exposure of the sheet to H_3O^+, it becomes softened and unstable, presumably due to hydrolysis of the Si-O-Si bridging bonds. Similarly, increasing temperature at close to neutral pH (pH 5.6), causes a weakening of the Si-O-Si bridging bonds, and removal of silicate units from the layers starts. The removal takes place at rough steps causing them to retreat. This observation is in agreement with Cave (2002) who reports that the dissolution stoichiometry approaches congruency in the neutral pH range. We determined the dissolution rate at pH = 5.6, T = 130 °C, and P = 10 bar to be about 5×10^{-7} mol/m^2s.

Acidic attack on micas and clays begins at the edges of the crystals and works inward. The contribution of the crystal basal planes to the dissolution process is usually considered to be relatively small and becomes apparent mainly in the last stages of dissolution (Zysset and Schindler, 1996; Rufe and Hochella, 1999; Bosbach et al., 2000). Another situation is possible when the basal surface plays a significant role in the dissolution process. For example, Huertas et al. (1999) stressed the important contribution of the kaolinite basal plane to the overall dissolution. According to our observations, in the alteration process in apophyllite at low pH both edges and the basal surface participate. The protons penetrate through surface defects into the interlayer space and initiate the ion-replacement process, that causes a K and Ca depleted residue and, eventually, the Si-O-Si bonds of the residue weaken and break. This mechanism in apophyllite is different from the ion-exchange in zeolites or the interlayer of 2:1 sheet silicates, in which the silicate sheets (or the framework in zeolites) are not protonated. For the hillock formation of apophyllite it is very likely that the terminal oxygen atoms of the silicate sheet are protonated to form Si-O-H groups, and thus the reaction bears a close relation to the acid hydrolysis of the octahedral layer in 2:1 sheet silicates (e.g., Kaviratna and Pinnavaia, 1994).

Thus, we can mark out a significant role of defect type and density in both the mechanism and the rate of apophyllite dissolution. Also the proton concentration in solution and temperature have a significant influence on the rate of dissolution of apophyllite. This applies to both processes: cation replacement and residue dissolution. In this respect apophyllite differs from some other sheet silicates. For example, in the case of biotite it was found that potassium release is very fast, at least in the beginning of the experiment, and it has a more or less constant rate which shows no trend as a function of pH (Malmström and Banwart, 1997). Newman (1970) has found some relationship between pH and K-release in biotite and phlogopite, however this dependence was not as strong as in case of apophyllite. This difference reflects the different interlayer linkage pattern in apophyllite as compared to micas and clays.

5. CONCLUSION

In the present work we studied the apophyllite (001) surface *in situ* in aqueous solutions with different pH (1.5 - 5.6) and at different temperatures. At low pH conditions, dissolution of apophyllite shows similarities to the dissolution of other sheet silicates (such as clays and micas). In a first stage of the acidic dissolution of clays and micas, interlayer cations are removed more rapidly than the silicate layers. This preferential release of interlayer cations has been attributed to a rapid ion-exchange reaction with protons (e.g., Newman, 1970; Malmström and Banwart, 1997). Some authors also reported an expansion effect in normally nonswelling minerals such as biotite and phlogopite by HCl solutions. This expansion was attributed to the occurrence of hydroxy interlayers (Kalinowski and Schweda, 1996).

Our observations point towards a different interpretation of the swelling in apophyllite. We suggest that due to the interaction of apophyllite with acidic solution, an ion replacement reaction between interlayer bridging ions and H_3O^+- ions takes place. However, it is unlikely, that the mono-valent hydronium ions can provide the charge density that is provided by Ca^{2+}-ions which are grouped closely together in the apophyllite interlayer. In view of the conclusion of Lagaly and Matouschek (1980) and Sogo et al. (1998) we conclude that the reaction involves a protonation of terminal oxygens of the silicate sheet to silanol groups in the interlayer. This leads to the reduction of attractive forces between the silicate layers and, therefore, to a larger distance between the silicate sheets than in pristine apophyllite thus stressing the fundamental difference between the structure of the hydrous interlayer in swollen clay minerals and in the hillock structure of apophyllite.

In spite of some structural similarities to zeolite minerals, apophyllite in general behaves as a typical phyllosilicate. In zeolites, the processes of adsorption and ion exchange do not lead to a desintegration of the framework. In apophyllite, the ion replace-

ment involves interlayer ions, which link silicate sheets together and which, therefore, are fundamental for sustaining the structural topology. Replacement of these topologically relevant ions eventually causes a disintegrative tendency of the structure. At present, a study of the reversibility of hillock formation in apophyllite is being conducted giving further insights into the interlayer mechanisms of reactions with aqueous solution. Also, a particular interest in this field is to study the possible incorporation of different types of ions into the apophyllite structure. Because of its remarkable structure, apophyllite seems to be a very promising mineral for such applications.

Acknowledgments— Funding for the construction of the HAFM and for conducting this project was provided by the Deutsche Forschungsgemeinschaft (DFG) and is gratefully acknowledged. We also wish to thank H.-J. Bernhardt for performing electron microprobe analysis and Ralf Dohmen for handling the RBS spectra. Furthermore, the authors are grateful to Roy A. Wogelius for editorial handling and improving the manuscript, to Barry R. Bickmore and an anonymous reviewer for helpful comments.

Associate editor: R. Wogelius

REFERENCES

Astilleros J. M., Pina C. M., Fernández-Diáz L., and Putnis A. (2002) Molecular-scale surface processes during the growth of calcite in the presence of manganese. *Geochim. Cosmochim. Acta* **66**, 3177–3189.

Bickmore B. R., Bosbach D., Hochella M. F. Jr., Charlet L., and Rufe E. (2001) *In situ* atomic force microscopy study of hectorite and nantronite dissolution: Implications for phyllosilicate edge surface structures and dissolution mechanisms. *Am. Mineral.* **86**, 411–423.

Bosbach D., Hall C., and Putnis A. (1998) Mineral precipitation and dissolution: *In-situ* microscopic observations on barite (001) with atomic force microscopy. *Chem. Geol.* **151**, 143–160.

Bosbach D., Charlet L., Bickmore B., and Hochella M. F. Jr (2000) The dissolution of hectorite: *In-situ*, real-time observations using atomic force microscopy. *Am. Mineral.* **85**, 1209–1216.

Cave L. C (2002) Apophyllite weathering and the aqueous geochemistry of a Karoo breccia pipe. Ph. D. thesis, Department of Geological Sciences, University of Cape Town.

Charistos D., Godelitsas A., Tsipis C., Sofoniou M., Dwyer J., Manos G., Filippidis A., and Triantafyllidis C. (1997) Interaction of natrolite and thomsonite intergrowths with aqueous solutions of different initial pH values at 25 degrees C in the presence of KCl: Reaction mechanisms. *Appl. Geochem.* **12**, 693–703.

Colville A. A., Anderson C. P., and Black P. M. (1971) Refinement of the crystal structure of apophyllite, I. X-ray diffraction and physical properties. *Am. Mineral.* **56**, 1222–1233.

Dunn P. J., Rouse R. C., and Norberg J. A. (1978) Hydroxyapophyllite, a new mineral, and a redefinition of the apophyllite group, I. Description, occurrences, and nomenclature. *Am. Mineral.* **63**, 196–199.

Frondel C. (1979) Crystalline silica hydrates from leached silicates. *Am. Mineral.* **64**, 799–804.

Hall C. and Cullen D. C. (1996) Scanning force microscopy of gypsum dissolution and crystal growth. *Aiche J.* **42**, 232–238.

Higgins S. R., Eggleston C. M., Knauss K. G., and Boro C. O. (1998) A hydrothermal atomic force microscope for imaging in aqueous solution up to 150°C. *Rev. Sci. Instrum.* **69**, 2994–2998.

Higgins S. R., Jordan G., and Eggleston C. M. (2002) Dissolution kinetics of magnesite in acidic aqueous solution: A hydrothermal atomic force microscopy study assessing step kinetics and dissolution flux. *Geochim. Cosmochim. Acta* **66**, 3201–3210.

Hillner P. E., Gratz A. J., Manne S., and Hansma P. K. (1992) Atomic-scale imaging of calcite growth and dissolution in real time. *Geology* **20**, 359–362.

Hochella, M. F., Jr., Rakovan J., Rosso K., Bickmore B. R., and Rufe E. (1998) New directions in mineral surface geochemical research using scanning probe microscopy. In *Mineral-Water Interfacial Reactions: Kinetics and Mechanisms, ACS Symposium Series*, **715** (ed. Sparks DL, Grundl TJ). Washington, DC 37–56.

Huertas F. J., Chou L., and Wollast R. (1999) Mechanism of kaolinite dissolution at room temperature and pressure. Part II: Kinetic study. *Geochim. Cosmochim. Acta* **63**, 3261–3271.

Jordan G. and Rammensee W. (1998) Dissolution rates of calcite (10(1)over-bar4) obtained by scanning force microscopy: Microtopography-based dissolution kinetics on surfaces with anisotropic step velocities. *Geochim. Cosmochim. Acta* **62**, 941–947.

Jordan G., Higgins S. R., Eggleston C. M., Knauss K. G., and Schmahl W. W. (2001) Dissolution kinetics of magnesite in acidic aqueous solution, a hydrothermal atomic force microscopy (HAFM) study: Step orientation and kink dynamics. *Geochim. Cosmochim. Acta* **65**, 4257–4266.

Joshi M. S. and Ittyachen M. A. (1967) Rotation of etch pits on the basal cleavages of apophyllite crystals. *Phyl. Mag.* **16**, 717–721.

Kalinowski B. E. and Schweda P. (1996) Kinetics of muskovite, phlogopite and biotite dissolution and alteration at pH 1–4, room temperature. *Geochim. Cosmochim. Acta* **60**, 367–385.

Kaviratna H. and Pinnavaia T. J. (1994) Acid hydrolysis of octahedral Mg^{2+} sites in 2: 1 layered silicates: An assessment of edge attack and gallery access mechanisms. *Clays & Clay Miner.* **42**, 717–723.

Kotai E. (1994) Computer methods for analysis and simulation of RBS and ERDA spectra. *Nucl. Instrum. Meth. Phys. Res.* **B85**, 588–596.

Lagaly G. and Matouschek R. (1980) The crystalline silicic acids from apophyllite, carletonite and gillespite. *N. Jb. Mineral. /Abh.* **138**, 81–93.

Malmström M. and Banwart S. (1997) Biotite dissolution at 25°C: The pH dependence of dissolution rate and stoichiometry. *Geochim. Cosmochim. Acta* **61**, 2779–2795.

Marriner G. F., Tarney J., and Langford J. I. (1990) Apophyllite group: Effects of chemical substitutions on the dehydration behaviour, recrystallization products and cell parameters. *Mineral. Mag.* **54**, 567–577.

Nagy K. L. and Blum A. E. (1994) *Scanning Probe Microscopy of Clay Minerals*. The Clay Minerals Society, Boulder, USA.

Newman A. C. D. (1970) The synergetic effect of hydrogen ions on the cation exchange of potassium in micas. *Clay Minerals* **8**, 361–373.

Pande D. R. and Vadrabade S. R. (1990) Etch pits on basal cleavage faces of apophyllite crystals. *Mineral. Mag.* **54**, 559–565.

Rivera A., Rodriguez-Fuentes G., and Altshuler E. (2000) Time evolution of a natural clinoptilolite in aqueous medium: Conductivity and pH experiments. *Microporous Mesoporous Mater.* **40**, 173–179.

Rufe E. and Hochella M. F. Jr (1999) Quantitative assessment of reactive surface area of phlogopite during acid dissolution. *Science* **285**, 874–876.

Shiraki R., Rock P. A., and Casey W. H. (2000) Dissolution kinetics of calcite in 0.1 m NaCl solution at room temperature: An atomic force microscopic (AFM) study. *Aquatic Geochem.* **6**, 87–108.

Sogo Y., Iizuka F., and Yamazaki A. (1998) Preparation and properties of layered silica and layered alumino-silica hydrate from natural apophyllite. *J. Ceram. Soc. Japan* **106**, 160–168.

Sposito G. (1984) *The Surface Chemistry of Soils*. Oxford University Press, Oxford, U.K.

Stipp S. L. S., Eggleston C. M., and Nielsen B. S. (1994) Calcite surface structure observed at micrographic and molecular scales with atomic force microscopy (AFM). *Geochim. Cosmochim. Acta* **58**, 3023–3033.

Teng H. H. and Dove P. M. (1997) Surface site-specific interactions of aspartate with calcite during dissolution: Implications for biomineralization. *Am. Mineral.* **82**, 878–887.

Theodossiu W., Misaelides P., and Godelitsas A. (2001) Investigation of fluorine distribution on the surface of acid-treated apatite single crystals using nuclear resonant reaction analysis. *Cryst. Res. Technol.* **36**, 1247–1251.

Yamamoto S., Sugiyama S., Matsuoka O., Kohmura K., Honda T., Banno Y., and Nozoye H. (1996) Dissolution of zeolite in acidic and alkaline aqueous solutions as revealed by AFM imaging. *J. Phys. Chem.* **100**, 18474–18482.

Zysset M. and Schindler P. W. (1996) The proton promoted dissolution kinetics of K-montmorillonite. *Geochim. Cosmochim. Acta* **60**, 921–931.